

## EFFECT OF AN EXTERNAL FLOW ON COMBUSTION IN A TRAPPED-VORTEX BURNER

**Farid C. Christo<sup>1\*</sup>, Graham J. Nathan<sup>2</sup>, and Richard M. Kelso<sup>2</sup>**

<sup>1</sup> Barbara Hardy Institute, University of South Australia, Mawson Lakes 5095, AUSTRALIA

<sup>2</sup> Centre for Energy Technology, Adelaide University, Adelaide 5055, AUSTRALIA

\*Corresponding author, E-mail address: farid.christo@unisa.edu.au

### ABSTRACT

This study examines the flow and flame characteristics of a trapped-vortex burner (TVB) under various external flow conditions. A detailed numerical study was carried out to explore and better understand the flow features that enable the burner to maintain flame stability under high-velocity co-flow and cross-flow conditions. Three-dimensional steady-state and time-dependent calculations are performed for a turbulent, reacting propane jet burning in air with a co-flow speed in the range  $5.5\text{ms}^{-1}$ – $27.7\text{ms}^{-1}$ . The calculations are repeated for the same velocity range with the burner model oriented in a cross-flow configuration. Among several two-equation turbulence models, the  $\kappa$ - $\omega$  SST turbulence model provided the best agreement against published experimental data, and therefore was used in all the calculations. The turbulence-chemistry interaction is modelled using the laminar-flamelet concept, with the propane chemistry represented using a kinetics mechanism with 31 species and 65 reactions.

The results identified two distinct combustion zones; an internal vortex-flame within the cavity of the burner and an external jet-flame anchored outside the cavity, consistent with experimental observations. The size and location of the internal vortex-flame was almost independent of the external flow conditions. The vortex-flame acts as a re-ignition source should the jet-flame experience localised extinguishment. This study provides a detailed insight into the turbulent mixing and combustion features of a TVB flame, and identifies the main flow characteristics responsible for enhancing its stability.

### NOMENCLATURE

$D_j$	fuel jet diameter	.....	mm
$D_{TVB}$	diameter of the burner cavity	.....	mm
$D_{FP}$	diameter of the flow partition	.....	mm
$D_{BB}$	diameter of the bluff-body plate	.....	mm
$H_{FP}$	flow partition vertical position	.....	mm
$L_{TVB}$	length of the burner cavity	.....	mm
$Re_j$	Reynolds number of the jet	.....	[-]
$\xi$	mixture fraction	.....	[-]
$\xi^2$	variance of mixture fraction	.....	[-]
$\kappa$	turbulent kinetic energy (TKE)	.....	$\text{m}^2\text{s}^{-2}$
$\varepsilon$	dissipation rate of TKE	.....	$\text{m}^2\text{s}^{-3}$
$\omega$	specific dissipation rate of TKE	.....	$\text{s}^{-1}$
$\chi$	scalar dissipation	.....	$\text{s}^{-1}$

### INTRODUCTION

Maintaining stability of turbulent flames under high strain rates is critical in most industrial combustion systems. It is an essential safety criterion and necessary for process stability and maximum thermal efficiency. Stable combustion systems have traditionally been based on designs that incorporate flow recirculation, generated either by mechanical or aerodynamic means, such as flow swirling devices, flame holders, bluff-bodies, sudden expansions and the like. The trapped-vortex burner (TVB) is an emerging concept that claims to enhance combustion stability, improve efficiency, lower emissions, and reduce pressure-drop across the combustor (Thévenin *et al.*, 2000, Renard *et al.*, 2000, Long *et al.*, 2006). Most of TVB applications have been primarily focusing on gas turbine combustors (Hendricks *et al.*, 2004, Di Nardo *et al.*, 2009, Patignani *et al.*, 2010) where physical cavities are created to confine and stabilise the combustion.

This study reports on a TVB application that is different to those designed for gas combustors, whereby its primary application being in ceremonial open flames. Maintaining flame stability in this environment is a challenging task considering that, unlike the vast majority of combustors, including in gas turbines, the shroud flow conditions are uncontrolled and unpredictable, with the flame having to withstand high wind speeds, strong gusts, thin shear layers from vehicles and rain. The design concept for this burner also has potential in other applications, such as pilot-flames or flare burners for industrial platforms that experience extreme winds and intense gust conditions. The design of the burner, developed and patented by Kelso *et al.* (2008) is primarily based on fundamental understanding and phenomenological knowledge of fluid dynamics and limited qualitative experimentation. The performance of the burner, particularly its flame stability in high wind speeds, has been demonstrated successfully in qualitative wind tunnel testing, and also on numerous ceremonial occasions, most notably as the torch burner for the Sydney 2000 Olympic Games. To the best knowledge of the authors however, there have been no published numerical studies or quantitative experiments on the flow or combustion characteristics of this burner. The objectives of this study therefore are; to model the flow and combustion fields of a trapped-vortex burner under various external flow conditions, and to identify the mechanisms responsible for its enhanced flame stability.

## BURNER MODEL

The geometry of the modelled trapped-vortex burner is based on a simplified version of the original design of Kelso *et al.* (2008). In this model configuration (Figure 1) the length of the fuel pipe ( $D_j = 1.1\text{mm}$ ) is  $35\text{mm}$ , in which  $14\text{mm}$  intrudes into the cavity of the burner. The length of the fuel pipe is sufficient to ensure a fully-developed flow as the jet enters the cavity. The internal diameter and length of the burner are;  $D_{TVB} = 29\text{mm}$ , and  $L_{TVB} = 39\text{mm}$ . A thin flow-partition  $21\text{mm}$  long and  $25.5\text{mm}$  ( $D_{FP}$ ) diameter is centred in the cavity, and vertically positioned  $4\text{mm}$  ( $H_{FP}$ ) above the fuel jet exit plane. A thin bluff-body plate of  $22\text{mm}$  diameter ( $D_{BB}$ ) with a  $3.5\text{mm}$ -diameter circular central port, is positioned  $12\text{mm}$  above the tip of the fuel pipe. The diameters of the flow partition and the bluff-body plate are less than that of the burner ( $D_{TVB}$ ), hence leaving  $1.75\text{mm}$ -wide gaps on each side. The outer gap is intended to allow ambient air to be entrained into the cavity for combustion and cooling, and the inner gap is intended as an air-fuel mixture outlet.

The computational domain for the burner includes the cavity and extends externally approximately two meters in the downstream and lateral directions. This is deemed an adequate distance for minimising numerical errors imposed by the proximity of pressure boundaries to the burner domain. A refined grid (mesh size of the order of  $0.1\text{mm}$ – $2\text{mm}$  to resolve flow in the fuel tube) is constructed in the cavity and the immediate region outside the TVB, growing gradually towards the outer boundaries (up to a mesh size of  $20\text{mm}$ ) of the computational domain.

For modelling the reacting flow, a mixture fraction ( $\xi$ ) conserved scalar concept allows decoupling of the chemistry terms and the flow field, hence significantly reducing the required computational resources. Chemical reaction rates are computed first (independently of the flow) and the relevant scalar properties are stored in look-up tables accessible by the flow solver. A skeletal mechanism deduced from the GRI 3.0 kinetics was used to represent the chemistry of the propane. It consists of 31 (minor, major and radical) species and 65 reactions. A reduced kinetics model is unlikely to affect the accuracy of predicting the overall distribution of temperature and species. It might have marginal effect on prediction of peak values of radical species. The flamelet combustion concept (Peters, 1986) is used. In this model the turbulent flame brush is modelled as an ensemble of discrete, steady laminar flames referred to as ‘flamelets’, each assumed to have the same structure as laminar flames in a simple counter-flow diffusion flame. The mean scalar properties ( $\phi$ ) are represented as a function of the instantaneous mixture fraction  $\xi$  its variance  $\xi'^2$ , and the scalar dissipation  $\chi$ ;  $\phi = \phi(\xi, \xi'^2, \chi)$ . The transport equation for the scalar dissipation includes a term that accounts for Lewis number effects. During the iterative calculations, turbulence-chemistry interactions are handled by solving transport equations for the turbulent kinetic energy ( $\kappa$ ), its specific dissipation rate ( $\omega$ ), mixture fraction ( $\xi$ ) and its variance  $\xi'^2$  ( $\xi'^2$  is used to compute turbulent scalar dissipation  $\chi$ ), for each computational cell. These values are then used to extract mean scalar properties from look-up tables of chemistry. The flow field properties are updated and iterations continue until convergence criteria are met. All calculations are performed using the commercial ANSYS FLUENT CFD package. A second

order discretisation scheme is used for all equations. Solution convergence is determined by ensuring all residuals of the transport equations drop below a pre-determined threshold and no longer changing with iterations. Grid-independence was evaluated using a dynamic mesh refinement in regions of high temperature gradient. This approach is more efficient than the conventional static mesh grid-independence analysis.

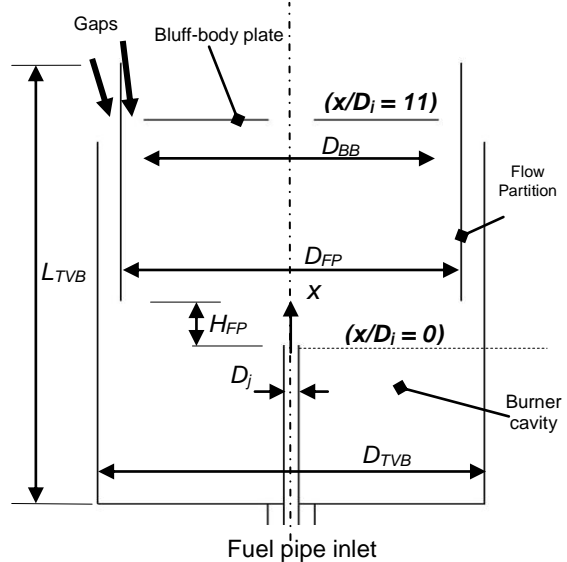


**Figure 1:** Geometry of the Trapped Vortex Burner (TVB) modelled in this study (Kelso *et al.*, 2008).

## RESULTS AND DISCUSSION

Computing the turbulence quantities as accurately as possible is critical when modelling reacting flows. This is due to the significant effects that fluctuations in the scalar field have on the mean flow and the mean chemical reaction rates. Selecting an appropriate turbulence model is therefore essential to ensure accurate predictions of temperature and species concentration fields in reacting flows. In this study, the performance of six two-equation turbulence models are evaluated; the standard  $\kappa$ - $\epsilon$  (SKE), renormalization group (RNG), the realizable  $\kappa$ - $\epsilon$  (RKE), modified  $\kappa$ - $\epsilon$  (MKE), Standard  $\kappa$ - $\omega$  (SKW), and  $\kappa$ - $\omega$  SST model (ANSYS, 2011). The modified  $\kappa$ - $\epsilon$  variant is effectively the standard  $\kappa$ - $\epsilon$  model but with a  $C_{\epsilon 1}$  constant in the dissipation rate equation of 1.6 instead of the commonly used value of 1.44. In previous modelling studies of inert and reacting free jets, the modified  $\kappa$ - $\epsilon$  model demonstrated superior accuracy in predicting the centreline velocity decay rate against other two-equation models (Dally *et al.*, 1998, Christo and Dally, 2005).

Due to insufficient quantitative experimental data for this specific burner, the calibration of the turbulence model is performed against data from an inert free jet experiment (Kwon and Seo, 2005). To reduce the computational resources, an axisymmetric model is used in the calculations of a free jet of air ( $Re_j = 3540$ ) issuing into a quiescent air. As shown in Figure 2, for the configuration without an external cross-flow or co-flow, the axisymmetric assumption does not have a significant effect on the accuracy of the predictions.

The rate of decay of the jet’s centreline velocity in the chamber, as predicted by all but one of the turbulence

models, exhibits a faster decay rate than the experimental data for a free jet (Figure 3). The only exception is the SKW model, which predicts weaker dissipation than the experiments.

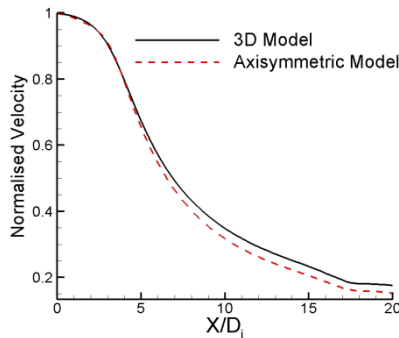


**Figure 2:** Axial centreline velocity of an inert jet ( $Re_j=3540$ ) as predicted by axisymmetric and full three-dimensional models. The velocity and distance are normalised by the exit velocity and nozzle diameter, respectively.

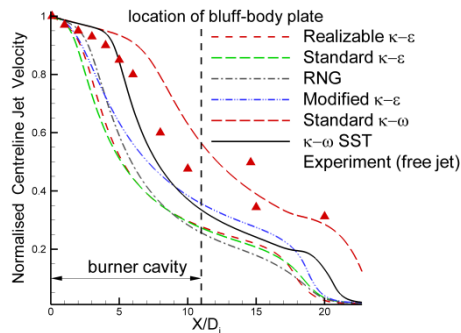


**Figure 3:** Axial centreline velocity decay of an inert jet ( $Re_j=5454$ ) in the trapped-vortex burner cavity as predicted by different turbulence models, compared with data obtained in a free-jet experiment,  $Re_j=5142$  (Kwon and Seo, 2005). The velocity and distance are normalised by the exit velocity and nozzle diameter, respectively.

Care must be taken in comparing the experiments and the models, since the confinement increases the spreading rate of a jet. The two versions of the  $\kappa-\epsilon$  model under-predict spreading in the near field, with the SKW exhibiting significant under-prediction. The modified  $\kappa-\epsilon$  prediction yields a higher spreading rate than the experimental data, which is qualitatively consistent with the effects of confinement. The  $\kappa-\omega$  SST model provides the closest predictions to the experimental data in the near-field (i.e. within the cavity domain), and therefore is used in all subsequent calculations. Perhaps surprisingly, the predictions of the standard  $\kappa-\epsilon$  model in the far-field ( $x/D_j > 15$ ) are reasonably close to the measured data, although it significantly over-predicts the decay-rate in the near-field, which is the region of interest in this study.

Although the turbulence models have a notable influence on the axial centreline decay rate of the jet, all of the models predict that the flow inside the cavity consists of several counter-rotating vortices, with key features being similar, as shown in Figure 4. However the flow pattern produced by the  $\kappa-\omega$  SST model (Figure 4c) resolves additional vortices adjacent to the flow partition and burner wall (marked by arrows for clarity). These vortices are apparently formed by the separation and roll-up of vorticity generated at the adjacent surfaces. Their presence

in the  $\kappa-\omega$  SST flow pattern may be due to the slightly higher dissipation rate of that model away from the near field of the jet, leading to a more rapid rate of boundary layer growth. In the absence of experimental confirmation of the flow structure, the  $\kappa-\omega$  SST model will be adopted for further analysis. Some qualitative flow observations (Kelso, 2012) are available which support the present flow patterns, especially the one calculated using the  $\kappa-\omega$  SST model.

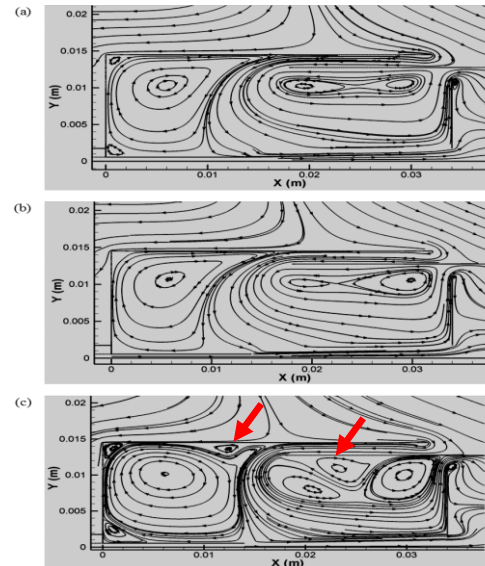


**Figure 4:** Streamlines of an inert jet ( $Re_j=5454$ ) injected into the trapped-vortex burner cavity, as predicted by; (a) standard  $\kappa-\epsilon$ , (b) realisable  $\kappa-\epsilon$ , and (c)  $\kappa-\omega$  SST turbulence model. (Arrows show the additional resolved vortices predicted by the  $\kappa-\omega$  SST model).

The use of an axisymmetric model for modelling reacting jets with external flows is not suitable because it cannot resolve three-dimensional flow effects, such as cross-flow or flow instabilities. Therefore, a full three-dimensional model is developed for modelling the reacting flow configurations. A pre-heated gaseous propane fuel (573K) is injected into the burner at a mean velocity of  $92\text{ m/s}$  ( $Re_j \approx 5400$ ) and turbulence intensity of 2%. The fuel flow rate ( $\sim 8.1 \times 10^{-5} \text{ kg/s}$ ) is kept unchanged for all the modelled reacting configurations. The chemistry of propane is represented in the model using a multistep kinetics mechanism that consists of 30 reactive species and 65 reactions. A flamelet library with multiple strained laminar flames is generated and stored in lookup tables. Three-dimensional steady-state calculations are performed for air co-flow ( $x$ -direction) velocities of  $5.5 \text{ ms}^{-1}$ ,  $11.1 \text{ ms}^{-1}$ ,  $16.6 \text{ ms}^{-1}$ ,  $22.2 \text{ ms}^{-1}$ , and  $27.7 \text{ ms}^{-1}$ . The calculations are repeated for the same velocity range for a cross-flow ( $y$ -direction) configuration.

The predicted flow structure in the TVB cavity for inert and reacting propane jets issuing into a still air environment, is shown in Figure 5. The figure indicates that combustion does not significantly alter the size or location of the vortices within the cavity. This is a highly desirable feature for a burner considering that heat release due to chemical reactions could generate strong flow dilation, causing the vortices to disintegrate or disappear altogether. Considering that these vortices act as a flame stabilisation mechanism, maintaining their stability is

essential to minimising flame instability or flame blow-out. However, Figure 5 (bottom) shows a significant flow outside the burner, which looks like a co-flow. This flow is an ambient air entrained by the momentum of the flame. Although the flow topologies of the inert and reacting cases are similar, the flame affects the flow pattern outside the bluff body, creating a large recirculation zone to form outside the bluff plate. This is completely consistent with experimental observation (Kelso, 2012).

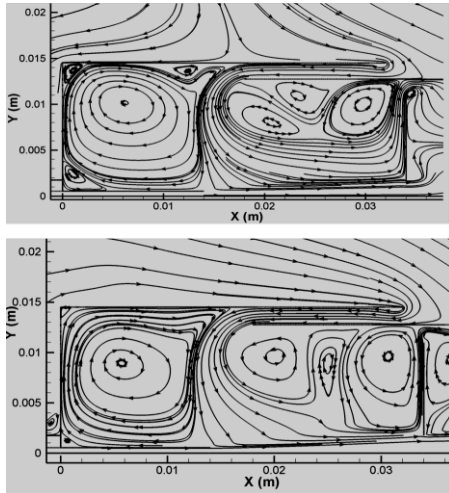


**Figure 5:** A comparison of flow structure (streamlines) inside the cavity of a trapped- vortex burner for; (top) an inert flow,  $Re_j = 3540$  and (bottom) a reacting propane jet,  $Re_j = 5400$ . The  $\kappa$ - $\omega$  SST turbulence model is used in both configurations.

To explore the effect of the turbulence models on the predictions for a reacting jet, the stoichiometric flame length is computed. It showed that the standard  $\kappa$ - $\epsilon$  predicts a shorter flame (by 4%) than the  $\kappa$ - $\omega$  SST model. This result is consistent with the previous observation (Figure 3) showing a faster decay-rate prediction of the centreline velocity by the standard  $\kappa$ - $\epsilon$  model. However, the overall flame sheet location and shape within and outside the cavity are similar for both turbulence models. This result reinforces an earlier observation (Figure 4) that turbulence models do not significantly alter the qualitative predictions of the flow structure (shape and location of vortices) and flame sheet.

The effect of external co-flow on the length of the flame, illustrated in Figure 6, shows a decrease in the flame length with increasing co-flow velocity. A similar trend is observed for the cross-flow configuration (Figure 7), which was also observed in laboratory experiments. However, the dependency of the flame length on the external flow velocity is different in both flow configurations, as highlighted in Figure 8. The figure shows an approximately linear correlation for the co-flow, but a non-linear dependency for the cross-flow configuration. The latter shows a steep reduction in the flame length with increasing the cross-flow velocity to  $5.5 \text{ ms}^{-1}$  followed by a slower rate of change.

The predictions (in both flow configurations) identified two distinct combustion zones; a vortex-flame that is formed within the cavity of the burner and an external jet-flame anchored outside the cavity. The vortex-flame plays a significant role in the stability of the jet-flame.

Experimental observations suggest that it pre-heats both the fuel and air entering the cavity, and provides hot gases (and unburnt fuel) for the external jet-flame through the central port of the bluff-body plate and the annular gap between the bluff body and the flow partition.

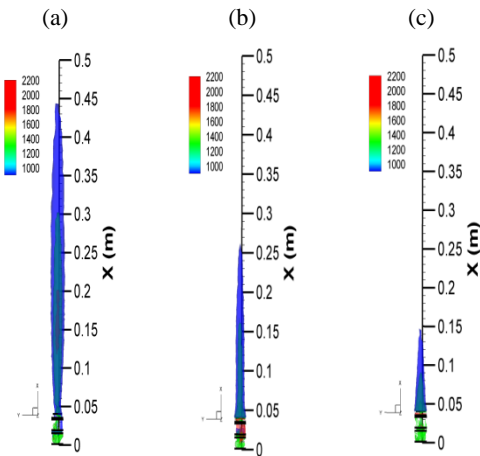


**Figure 6:** Flame length and shape represented as contours of temperature (K) of a propane jet of a trapped-vortex burner, with air a co-flow velocity of; (a)  $5.5 \text{ ms}^{-1}$ , (b)  $16.6 \text{ ms}^{-1}$ , and (c)  $27.7 \text{ ms}^{-1}$ .

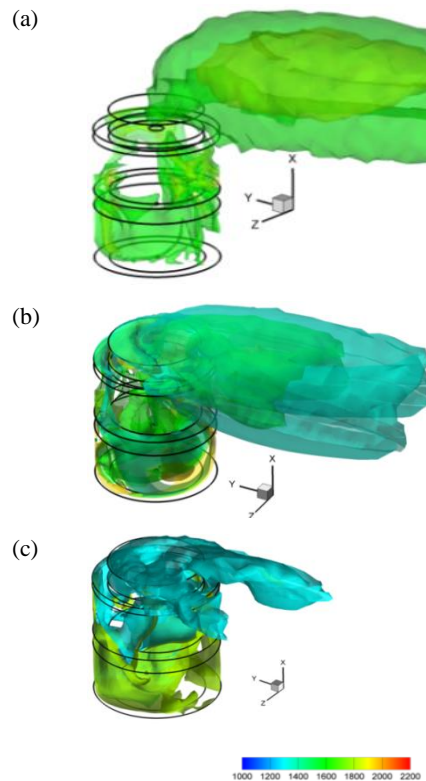


**Figure 7:** Flame length and shape of a propane jet of a trapped-vortex burner represented as temperature contours (K) with air cross-flow (from left) velocity of; (a)  $5.5 \text{ ms}^{-1}$  (b)  $16.6 \text{ ms}^{-1}$  and (c)  $27.7 \text{ ms}^{-1}$ .

It is interesting to observe that the temperature (typically  $\sim 900\text{K}$ ), the fuel mass fraction ( $\sim 0.5$ ), and the mass flow rates of gases passing through the bluff-body port, are almost independent of the external (co- or cross-) flow

velocity. The generation of stable vortices in the cavity and the continuous supply of pre-heated fuel and hot gases through the bluff-body port enhance the stability of the jet-flame across all conditions investigated here. The vortex-flame can also be expected to provide an immediate and consistent ignition source for the jet-flame should it experience intermittent blowout, as was observed in experiments.

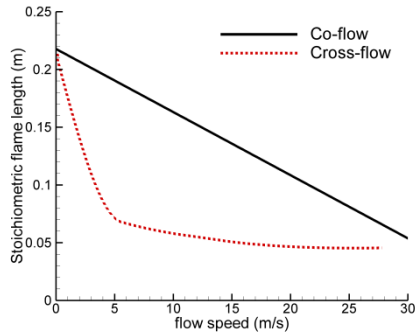


**Figure 8:** Stoichiometric flame length ( $m$ ) against external flow velocity ( $ms^{-1}$ ) for co-flow and cross-flow configurations.

The shapes of both the vortex-flame and the jet-flame were calculated to be asymmetrical under a cross-flow (Figure 7) for all cross-flow speeds. This is consistent with observations and with expectation, since a cross-flow alters the pressure distribution across the chamber and the spatial distribution of the entrained ambient air through the annular gap at the top of the burner. However, under a co-flow, an inspection of Figure 6 shows that the temperature contours of the jet-flame remain symmetrical irrespective of the co-flow speed. However, a small, but noticeable asymmetry is predicted in the vortex-flame for all co-flow speeds. It was tentatively postulated that this asymmetry is induced by the sudden expansion of the fuel jet as it enters the cavity causing flow instability. Such conditions could lead to a Coanda effect, i.e. the jet attaching itself to one side of the cavity (Abramson *et al.*, 2009, Zha *et al.*, 2005), or an initiation of a precessing motion of the jet in the cavity (Nathan *et al.*, 1998, Mi *et al.*, 1995). This is a possible outcome but is unlikely to occur in this configuration because the expansion ratio is too small and the cavity is too short. Another possible cause is emerging instability of the jet as it impinges on the bluff plate, leading to an asymmetry in the internal vortex pattern, thereby feeding back to the jet exit. To explore a more plausible explanation, further modelling is presented and discussed in the next paragraph.

To investigate the flow instability and identify its contribution to the observed flow asymmetry in the cavity, time-dependent calculations were performed for the co-flow configuration using an unsteady solver with integration time-steps of  $1 \times 10^{-5}$  sec. This time scale is approximately one-tenth of the estimated mean residence time of a fuel particle in the cavity. The results of the unsteady calculations (Figure 9) show similar overall flow and combustion patterns to those observed for the steady-state calculations, namely the existence of an internal vortex-flame and the external jet-flame. The figure shows contours of turbulent kinetic energy, temperature and molar concentration of water vapour, at three time intervals of  $0.1ms$ ,  $0.6ms$ , and  $1.2ms$ . The symmetrical profile of the turbulence field is evident inside and outside

of the cavity. This outcome indicates that the sudden expansion of the fuel jet does not induce instability in the flow; the velocity (not shown due to space constraints) and the turbulence fields remain symmetrical at all time-intervals. This is particularly obvious in the turbulent kinetic energy contours (Figure 9), which represents a stable and symmetrical fuel jet. The asymmetry is observed only in the temperature and the species fields inside the cavity, which persists at all time intervals. However, this asymmetry is stable with no evidence of the vortices rotating in any direction inside the cavity (see  $H_2O$  contours in Figure 9).

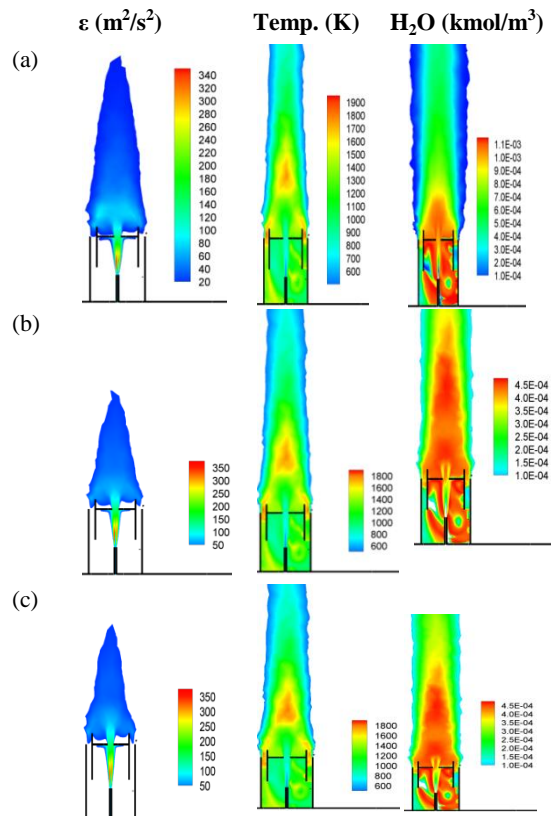


**Figure 9:** Contours of turbulent kinetic energy ( $m^2/s^2$ ), temperature (K), and water vapour molar concentration ( $kmol/m^3$ ) for a co-flow velocity of  $27.7 ms^{-1}$ , at various time intervals (a)  $0.1ms$ , (b)  $0.6ms$ , and (c)  $1.2ms$ .

Again, this observation indicates that the asymmetry is not related to instabilities in the flow (velocity or turbulence) fields. The most likely explanation for this asymmetry is numerical inaccuracies related to data interpolation from the flamelet library. Nonetheless, the overall effect of the asymmetry in the cavity on the jet-flame is negligible for these conditions. A closer examination of the profiles and scales of the temperature and  $H_2O$  molar concentration (Figure 9) at different time intervals indicates that the flame is calculated to pulsate along the axial direction of the flow (while retaining its symmetry in the other directions). Considering the high velocity ( $27.7 ms^{-1}$ ) of the co-flow, axial flame pulsation is not unusual behaviour, nonetheless the flame remains attached to the burner. However flame pulsation is not evident for the vortex-flame inside the cavity. These results are another demonstration of the strength of this TVB design in maintaining a stable and symmetrical jet-flame regardless of minor combustion asymmetry inside of the cavity.

Evaluation of the  $\text{NO}_x$  emission from the burner is carried out using a post-processing approach. This model solves a transport equation for nitric oxide (NO) concentration, as a major precursor for  $\text{NO}_x$  emission, integrated with velocity, turbulence, temperature, chemical species and radical fields that are already established by the flow solver. The model computes the thermal and prompt emissions of NO. Thermal  $\text{NO}_x$  is formed by the oxidation of atmospheric nitrogen present in the combustion air. Its formation rate is determined by a set of highly temperature-dependent chemical reactions (Zeldovich mechanism).

The Prompt (Fenimore)  $\text{NO}_x$  is produced by fast reactions at the flame front, and pertains to the specific combustion environment, such as in low-temperature, fuel-rich conditions and where residence times are short. The calculations predict that the rate of production of NO by thermal pathways is significantly larger (by a factor of 104) than the prompt NO mechanism. The maximum predicted concentration of NO (not shown due to space constraints) in a still-air environment, and that for a co-flow at  $27.7\text{ms}^{-1}$ , are  $220\text{ppm}_v$ , and  $14\text{ppm}_v$ , respectively. These peak values coincide with the locations of the highest gas temperature, hence the dominance of thermal NO formation over the prompt mechanism. Along the stoichiometric flame sheet, the maximum concentration of NO for the still-air and the co-flow configuration are  $30\text{ppm}_v$  and  $\sim 1\text{ppm}_v$ , respectively. Considering that this jet-flame is in an open combustion environment, correction of the computed NO to a specific oxygen level is not relevant. Excessive CO molar concentration (23%) is predicted in the cavity for both flow conditions. However, the maximum CO level within the core region of the jet-flame is around 7%, with emissions of less than 2% CO on the flame sheet boundary. Overall, the results show low NO emissions but the high level of CO emission warrants further investigation.

## CONCLUSION

The numerical models were found to give reasonable agreement with the limited available experimental data and good qualitative agreement with observations. A range of models was also found to identify similar qualitative flow features, demonstrating the robustness of these features and providing some confidence in their reliability.

Also, while the choice of turbulence model has a noticeable effect of the quantitative decay rate of the jet's centreline velocity, it only had a marginal influence on the predicted shape and length of the jet-flame. The length of the jet-flame was found to decrease approximately linearly with increased co-flow velocity. However the flame-length dependency in a cross-flow configuration is non-linear, showing the flame length to decrease drastically in a cross-flow of  $5.5\text{ms}^{-1}$ , but to marginally decrease further for higher velocities. The shape of the jet-flame retains its symmetry irrespective of the co-flow velocity; however the combustion field inside the cavity exhibits a stable, but asymmetrical temperature and species profiles. Analysis of the cause of the asymmetry points to numerical inaccuracies in the data interpolation from the flamelet library. However, there are no effects of this asymmetry on the stability of the jet-flame. In addition, time-dependent calculations have shown the co-flow to induce axial pulsation of the jet-flame, but without affecting its

symmetry in the other directions, and with the flame remaining attached to the cavity at all times.

The presence of a stable, shielded vortex-flame in the cavity is consistent with experimental observations and explains the maintenance of a highly stable jet-flame for a wide velocity range ( $5.5\text{ms}^{-1} - 27.7\text{ms}^{-1}$ ) of co-flow and cross-flow. The vortex-flame plays an important role in the stability of the jet-flame; it preheats the fuel and the oxidiser and provides a constant re-ignition source for the jet-flame, which further enhances its stability.

## REFERENCES

- THÉVENIN, D., RENARD, P.H., FIECHTNER, G.J., GORD, J.R., and ROLON, J.C., "Regimes of non-premixed flame-vortex interactions", Proc. of the Combustion Institute, 2000: Vol. 28, pp. 2101-2108.
- RENARD, P.-H., THÉVENIN, D., ROLON, J.C., and CANDEL, S., "Dynamics of flame/vortex interactions", Progress in Energy and Combustion Science, 2000, 26 (200) 225-282.
- LONG, E. J., HARGRAVE, G.K., JARVIS, S., JUSTHAM, T., and HALLIWELL, N., "Characteristics of the interaction between toroidal vortex structures and flame front propagation", Journal of Physics: Conference Series (2006) 45, 104-111.
- HENDRICKS, R.C., SHOUSE, D.T., ROQUEMORE, W.M., BURRUS, D.L., DUNCAN, B. S., RYDER R.C., BRANKOVI A., LIU N.-S., GALLAGHER, J.R., and HENDRICK, J.A., Experimental and Computational Study of Trapped Vortex Combustor Sector Rig with Tri-Pass Diffuser, NASA/M - 2004-212507, (2004).
- DI NARDO, A., CALCHETTI, G., MONGIELLO, C., GIAMMARTINI, S., and ROFOLONI, M., CFD Modelling of an Experimental Scaled Model of a Trapped Vortex Combustor, Proc of the European Combustion Meeting, 2009.
- PATRIGNANI, L., LOSURDO, M., and BRUNO, C. Numerical studies of the integration of a Trapped Vortex Combustor into traditional combustion chambers, Journal of the International Flame Research Foundation, (2010).
- STUGRESS, G.J., and HSU, K.-Y., Combustion Characteristics of a Trapped Vortex Combustor, Proc. Gas Turbine Engines Combustion, Emissions and Alternative Fuels", Lisbon, Portugal 12-16 October, 1998.
- KELSO, R. M., LANSPEARY, P.V., NATHAN, G.J., HILL, S.J., PARHAM, J.J., KELLY, G., CUTLER, P.R.E., and BUDRULHISHAM, M.G., Fluid Mixing Device, US Patent 7,410,288 B1, (2008).
- PETERS, N., "Laminar Flamelet Concepts in Turbulence Combustion", Proc. twenty-first Symposium (International) on Combustion, The Combustion Institute, 1986, pp. 1231-1250.
- ANSYS@FLUENT, Release 14.0, Chapter 4 Turbulence, ANSYS, Inc. (2011).
- DALLY, B.B., FLETCHER, D.F. and MASRI, A.R., Combust. Theory Modelling 2 (1998) 193-219.
- CHRISTO, F.C. and DALLY, B.B., "CFD Modelling of MILD Combustion using Detailed Chemical Kinetics", Combustion and Flame, 142 (2005) 117-129.
- KWON, S.J. and SEO, I.W., "Reynolds number effects on the behaviour of a non-buoyant round jet", Experiments in Fluids (2005) 38:801-812.
- KELSO, R.M., private communications (2012).
- ABRAMSON, P., VUKASINOVIC, B., and GLEZER, A., Fluidic Control of Steering Aerodynamic Forces on Axisymmetric Bodies using a Mid-Body Cavity, AIAA-2009-4276.
- ZHA, G. , CARROLL, B.F., PAXTONZ, C.D., CONLEYX, C.A., and WELLS, A., High Performance Airfoil Using Co-Flow Jet Flow Control, AIAA Paper 2005-1260.
- NATHAN G.J., HILL S.J., and LUXTON R.E. (1998) An axisymmetric 'fluidic' nozzle to generate jet precession. J. Fluid Mech., 370, pp.347-380.
- MI J., NATHAN G.J., and LUXTON R.E. (1995) Mixing characteristics of a flapping jet from a self-exciting nozzle. Flow, Turbulence & Comb., 67, pp.1-23.